Experimental determination of H_2 mass stopping powers for low-energy electrons

M. Zawadzki[1,2,*] and M. A. Khakoo[1]

[1]*Department of Physics, California State University, Fullerton, California 92831, USA*

[2]*Atomic Physics Division, Department of Atomic, Molecular and Optical Physics, Faculty of Applied Physics and Mathematics, Gdańsk University of Technology, ulica Gabriela Narutowicza 11/12, 80-233 Gdańsk, Poland*

(Received 8 January 2019; published 22 April 2019)

We present experimental mass stopping powers of electrons in gaseous H_2 obtained with an electron time-of-flight spectrometer, for the incident electron energy range of 11 to 25 eV. In our procedure, the average energy loss is derived from conversion of the measured electron time-of-flight spectra into equivalent electron energy-loss spectra. Our present results are compared with the only available experimental measurement and with theoretical models. The measurements are a significant improvement to the available experimental data to date.

DOI: 10.1103/PhysRevA.99.042703

I. INTRODUCTION

Any accurate experimental determination of mass stopping powers of electrons in a target species requires it to be made by an instrument that is able to (i) measure the complete differential electron scattering energy-loss spectrum, including the ionization continuum, that is induced by electron collisions with the target and (ii) measure it all with as close to a unity detection efficiency as possible. Since our present apparatus was able to do this for gaseous H_2, we are reporting these measurements here. The experimental setup has been reported in two earlier papers [1,2] on H_2. These measurements were tested for transmission properties of the apparatus using benchmark He data from Ref. [3] plus theory [1,2]. Here, we provide a detailed account of our determination of experimental mass stopping for gaseous H_2. Further on, we will discuss the need for stopping power measurements and the (markedly involved) analysis that has to be made to derive them from the experimental data.

Molecular hydrogen, the simplest molecule, has been the topic of extensive collision studies both theoretically as well as experimentally [1,2,4–8]. H_2 is a prevalent species in natural and manmade plasmas, which are important to the study of universal phenomena such as stellar emission, planetary aurorae, fusion, and formation of H_2O and life [9]. It is therefore fundamentally important to investigate this molecule as a first step before developing further models which concern more complex molecular systems, e.g., the diatomics N_2, CO, O_2, and the triatomics H_2O, CO_2, etc., which are important in planetary and life chemistry. In particular, the interaction of high-energy particles such as x rays, protons, ions, and electrons in solid-state materials, e.g., living tissue, leads to the copious production of secondary electrons. Over the turn of the millennium, it was recognized that the low-energy secondary electrons produced by ionizing radiation impinging on tissue matter, with kinetic energies below 50 eV, play an important role in the fragmentation of DNA [10,11] by dissociative electron attachment of these electrons to base pairs and backbone sites in the DNA, and hence affecting biological processes in living tissues. Theoretical methods, for example the *R*-matrix model [12], the convergent close-coupling (CCC) model [13], and exterior complex scaling [14] have been very successful in providing accurate collision parameters for low-energy electron scattering from atoms, but for electron collisions with molecules, theory has had a more difficult task. This is because of the complexity of having to cope with the increased number of channels in molecular structure, which, apart from electronic excitation and ionization, has to include rotational, vibrational, and dissociation channels. Consequently, electron-molecule collision theory has not computationally progressed to the same level of completion as electron collisions in atoms, at low-energy where interchannel couplings are very significant [2,15]. Present electron-molecule scattering models, e.g., the *R*-matrix model [16] or Schwinger multichannel model [17], can tackle only a limited number of electron-molecule scattering channels. However, the recent breakthrough CCC model of the Curtin University group [15] has provided accurate electron-H_2 cross sections, which were extended to the calculation of mass stopping powers for electrons on H_2 [18].

The low electron impact energy (E_0) range covered in the present measurements ($E_0 < 25$ eV) includes the region where the formation of molecular resonances [19–21] occur. In contrast to high-E_0 electrons, for which electron scattering can be predicted by generalized models with a reasonable accuracy, low-E_0 electron scattering has to be analyzed, as aforesaid, within a close-coupling formalism which includes electronic interchannel coupling and thus gives attention to the interaction of the scattering electron with a coupled electronic structure of the target, which includes the vibrational and rotational structure. The description of electron-molecule scattering at that detailed close-coupling level involves inclusion of a prohibitive number of collision channels to do precise numerical calculations of cross sections. As computers get more sophisticated and their memory gets increasingly faster

*mzawadzki@fullerton.edu

and larger, it becomes possible to solve electron-molecule scattering problems with increasing numerical detail and, consequently, better accuracy. As a consequence, presently reliable experimental electron-molecule cross-section data are needed for testing such theoretical models to advance them.

A useful parameter obtained from collision studies, which pertains to the attenuation of charged particles in media and quantifies the average (linear) rate of energy loss of a charged particle, is known as stopping power (SP). The SP is of fundamental importance in biomedical dosimetry, radiation physics, chemistry, medicine, and biology [22,23] involving neutrons, protons, x rays, and electrons. The SP provides the rate of energy loss per unit path length of the projectile particle in a medium, e.g., organic tissue, or liquid or gaseous media. Further, electron-H_2 SPs are of interest in astrophysics as H_2 is the most abundant molecule in the universe [24]. When SP is divided by the density of the absorbing medium, we obtain the mass stopping power (MSP). The MSP for low-energy electrons traveling in gaseous H_2 is the subject of the present work. Although the MSPs are widely used in many fields, they are not readily available experimentally. This is because in these measurements the complete electron energy-loss spectrum should be measured, and the spectrum should be corrected for instrumental transmission effects. Hence, presently, theoretical calculations have provided most of the MSP estimates.

Experimental MSP determinations are rare. To our knowledge, there presently exists only one experimental MSP measurement of electron-H_2 scattering. It was performed by Munoz *et al.* [25]. As aforementioned, any experiment that aims to determine accurate MSPs must collect all scattered electrons and discriminate them as a function of energy loss without incurring detector efficiency deficits. The Munoz *et al.* measurements were conducted in the energy range 15–5000 eV using a conventional electrostatic electron spectrometer (CES), and weight integrating the spectrum to determine the mean energy loss $\langle E_L \rangle$. However, there are several problems with energy-loss spectrometers that need to be factored in to produce accurate MSPs. The transmission of the spectrometer should be well characterized or, even better, a constant as a function of energy loss, E_L. Also, care should be taken in handling the ionization continuum in which the emitted electron signal further adds to the scattered electron signal in the energy-loss spectrum. In the case of Ref. [25] (the only other MSP experiment presently available), the ionization continuum was not properly handled as will be expounded further.

In the past, the evaluation of the electron MSPs for electron scattering from H_2 has been investigated by many theoretical studies at high-E_0 values. Here, interchannel coupling can be neglected and perturbative calculations applied. At high E_0, the well-known Bethe-Born theory [26,27] gives good agreement for charged particles with the experimental results at these high incident energies. Different extensions of the Bethe formula have been tested in order to also bring quantitative improvement for a different range of energies. Sugiyama [28] and Gumus [29] have obtained MSP values in the Bethe-Born theory for low and intermediate electron energies using a modified Rohrlich and Carlson model [30]. Different estimations of MSPs have included theoretical studies (using various versions of the Bethe theory) by Spencer and Pol [31], Peterson and Green [32], Takayanagi and Nakata [33], Dalgarno *et al.* [34], and Miles *et al.* [35]. The added problem of accurately evaluating electron-H_2 MSPs in the low-energy range comes from the fact (mentioned earlier) that at these energies, interchannel coupling requires a complete set of electron impact cross sections for all important discrete and continuum coupled channels to be taken into account. We note that Fursa *et al.* [18] have provided a low-energy theoretical MSP model, using their successful CCC model for H_2, which takes this into account.

In the present work, we have measured time-of-flight (TOF) electron scattering spectra and used them to provide experimental MSP of electrons in H_2 in the low-E_0 range, where there is sparse experimental data available. An important merit of the TOF method over the CES method is that the presence of electron focusing in various lens elements in CESs (altering transmitted electron trajectories) and its absence in TOF detectors (which does not alter electron trajectories) means the transmission of the TOF spectrometer is constant across the spectrum, whereas it is not in CESs. This also provides a magnetic field in the TOF experiment that is below 2 mG in the experimental chamber, but also below 5 mG or so for CES experiments. The spectra analyzed to determine the H_2 MSPs were taken at $E_0 = 11$ to 25 eV, for scattering angles θ of 20° to 130°. We note that above the ionization potential of H_2 at 15.43 eV [36], corrections need to be made for the detection of the electrons emitted from ionized H_2 molecules (continuum electrons) by spectrometers. We have also attempted to deal with the ionization continuum to correct it for detection of continuum electrons, a fact that is not taken into account in [25]. This is discussed in detail in the next section.

II. EXPERIMENT

The experiment was performed on a constructed time-of-flight spectrometer, consisting of an intense energy unselected pulsed electron gun and a time-of-flight (TOF) analyzer (see Fig. 1).

The apparatus and procedure used have been described in detail elsewhere, e.g., in the work of Zawadzki *et al.* [2], so only a brief summary of it is given here. The electron scattering experiment consisted of a pulsed electron gun which produced a collimated electron beam incident onto a collimated gas target effusing perpendicularly from a sooted molybdenum hypodermic needle of length 2.25 cm and outer and inner diameter of 1 and 0.8 mm, respectively. The needle was mounted on a magnetically free servomotor assembly, which rotated the needle in alignment (signal + background) and out of alignment (background) with the electron beam [37], at the center of a precise rotation platform on which the TOF tube was mounted. The TOF tube was aligned to view the center of the collision region which was about 6 to 8 mm above the end of the needle. The electron gun employed a dc current heated hairpin tungsten filament, with an energy width of about 400 meV full width at half maximum. This gun provided a 1–5 nA peak electron current pulsed electron beams with a 500 kHz repetition rate. The width of the electron pulse was between 2 and 3.5 ns as the electron pulse traveled through the interaction region. The pulsed electron

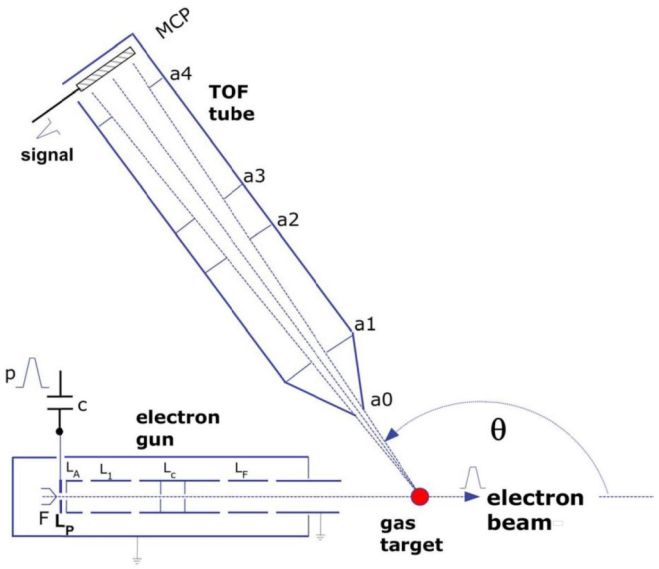

FIG. 1. A simplified schematic diagram (not to scale) of the TOF spectrometer. The collimated target gas (•) emanates out of the page. The nanosecond pulsed electron gun crosses the gas at a right angle. The TOF tube (heated to about 80 °C) is placed on a precise rotation platform and is able to detect the scattered electron at scattering angles (θ) of 20° to 135°. Electrons are detected by a triple-sandwich Z-stack microchannel plate (MCP) detector. The pulsed electrons are produced by capacitively pulsing (p) a reversed biased lens L_P. L_A, L_1, L_c, L_F are the anode lens, anode coupling lens, collimating lens, and focusing lens, respectively. The a1 to a4 are the collimating apertures in the TOF tube. For detailed setup and discussion, see Ref. [2].

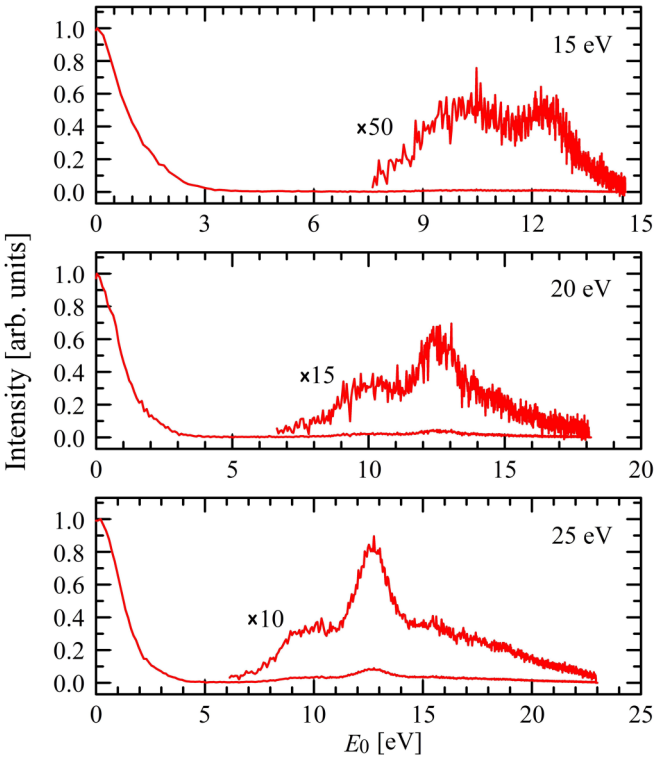

FIG. 2. Background-subtracted energy-loss spectra of 15, 20, and 25 eV electrons for H_2 at scattering angle of $\theta = 90°$. For clarity, the inelastic signal is magnified.

beam is produced by pulsing a negatively biased lens (LP in Fig. 1) placed in between the filament and an extracting anode, so that the voltage goes positive for a short time of about 2 ns and allows a burst of electrons to transit down the gun to the collision region using a precision 0–40 V pulser [38], wired in a 50 Ω coaxial circuit. A delayed coincidence circuit with a timing window of 200 or 500 ns was used to detect elastically and inelastically scattered electrons. The TOF displacement from the collision region to the MCP detector is 23.9 cm. By utilizing 40-inch-diameter Helmholtz coils, separated by 23 inches plus a 1.25-mm-thick μ-metal shield (with appropriate end caps) on the inner walls of the vacuum chamber, the magnetic field in the collision region was reduced to less than ±2 mG. This was crucial to satisfy the requirement for constant transmission of the TOF system without deflection of the slow electrons by the Earth's magnetic field. The chamber was pumped by three clean turbo pumps, reaching a base pressure of 1×10^{-7} Torr and the TOF tube was baked to further ensure it stayed clean. The TOF scale calibration was enabled using the $b\,^3\Sigma_u^+$ excitation feature at 10.19 eV and the $C\,^1\Pi_u$ excitation peak at 12.57 eV energy loss. In addition, this calibration was performed using time delay between UV photons (TOF = 0 ns) and the elastic peak. Knowing the absolute TOF timescale, we can transform the TOF scale into an energy-loss scale using the formula for E_L in eV as

$$E_L = E_0 - \frac{162\,413}{t^2} = E_0 - E_R, \qquad (1)$$

where t (ns) is the TOF of the electron (ns) and the TOF measures E_R, the residual energy of the scattered electron, i.e., for an E_0 of 15 eV the residual energy of the $b\,^3\Sigma_u^+$ feature at $E_L = 10.19$ eV, E_R would be at 4.81 eV and produce a TOF t value of 183.7 ns. This formula requires a very small correction for the exponentially rising grid-screened positive bias of the MCP front (+300 V with respect to ground) which only adds ≈1 to 0.5 ns to t, and this is done numerically via the laboratory computer in our conversion of the measured t to E_L. Once the energy-loss spectrum has been determined, we can calculate the MSP.

The TOF differential cross-section (DCS) scattering data were taken at E_0 values of 11, 11.5, 12, 12.5, 13.5, 14, 15, 15.5, 16, 17.5, 20, and 25 eV and are detailed in [2]. These were obtained by normalizing the elastic scattering feature in the TOF spectra to the elastic DCSs obtained from Muse *et al.* [39], again discussed in [2]. Figure 2 shows a typical energy loss spectra for 15, 20, and 25 eV incident electron energy recorded at $\theta = 90°$. The typical operating energy-loss spectra reveal a few distinctive features: elastic peak centered at 0 eV, $b\,^3\Sigma_u^+$ state centered at 10.19 eV, higher bound-state transitions centered at 12.57 eV, and the ionization signal for energies above the ionization threshold. The latter peak became more pronounced for higher impact energies.

III. DETERMINATION OF THE MASS STOPPING POWER

The mass stopping power is defined by the well-known formula

$$\mathrm{MSP} = \frac{1}{\rho}\frac{dE}{dx} = \frac{N_a}{M}\langle E_L\rangle\,\sigma_{\mathrm{inel}}, \qquad (2)$$

where N_a is Avogadro's number, M is the molar mass of the molecule, in this case for $H_2 = 2.016$ g/mol, $\langle E_L \rangle$ is the mean inelastic energy loss, σ_{inel} is the integral inelastic cross section in a.u., and ρ is the density of gaseous H_2, and is not needed here as it is on the left-hand side of Eq. (3), which is not used for MSP determinations as the most-right-hand part of Eq. (3) is used here. The determination of the most-right-hand parts of this equation follows:

$$\sigma_{inel}(E_0) = 2\pi \int_0^{\pi} \frac{d\sigma_{inel}}{d\Omega}(E_0, \theta) \sin\theta d\theta. \quad (3)$$

The values of our inelastic DCSs ($= \frac{d\sigma_{inel}}{d\Omega}$) have been determined from [1,2]. $\langle E_L \rangle$ was obtained from the energy-loss spectra. $\langle E_L \rangle$ is essentially a DCS weighted mean of the E_L values across the energy-loss spectrum and is given by

$$\langle E_L \rangle = \frac{2\pi \int_{E_{L\min}}^{E_{L\max}} dE_L \int_0^{\pi} \frac{d\sigma}{d\Omega}(E_0, \theta, E_L) E_L \sin\theta d\theta}{2\pi \int_0^{\pi} \frac{d\sigma}{d\Omega}(E_0, \theta) \sin\theta d\theta}. \quad (4)$$

We note here the lengthy analysis that is required to determine $\langle E_L \rangle$. Another important note to make here is that above the ionization energy (I_p) of H_2 at 15.43 eV [36], the spectrum contains not only contributions from scattered energy-loss electrons, but also continuum electrons which add to the "E_L" signal, and so the detected ionization energy-loss continuum is raised due to continuum electrons. To counteract this to a first order, we have reduced the continuum by a factor of 2, as this tends to make our ionization DCSs in significantly better agreement with theory, which is discussed, justified, and illustrated in [2]. At E_0 close to I_p (e.g., $E_0 = 17.5$ eV), the ionization continuum makes up ≈10% of the total inelastic scattering and this correction is not significant, but at our highest E_0 of 25 eV, the ionization contribution is ≈20% to 25% of the total inelastic DCS [2]. Fortunately, the reduction of the ionization contribution by the factor of 2 makes for a meaningful and good correction, as at the higher E_0 values elevated from I_p, reduced postcollision interaction (PCI) causes the continuum and scattered electrons to have approximately the same angular distributions. The well-known effect of PCI at near-threshold energies above I_p causes the (faster) E_L scattered electron (which peaks in the forward direction [2]) to push back the slow continuum electrons into the backward direction, making the angular distributions of the E_L electrons significantly different from the continuum electrons.

The experimental data from the TOF detector were analyzed in order to obtain the meaningful results that were used to determine the MSP. The weighted mean excitation energy was derived for each angle ($\theta = 20^\circ$ to 130°). At any given E_0 when the $\langle E_L \rangle$ for all θ was averaged, it fluctuated <0.26 eV, corresponding to a ≈2.5% standard deviation error. The integration of the inelastic cross section ranging from $\theta = 0^\circ$ to 180° to obtain integral inelastic cross sections (ICSs), required us to implement an additional extrapolation of the DCSs to the low-θ and large-θ regions outside of the measurement regions of the TOF detector of $20^\circ > \theta > 130^\circ$. For these small and large θ, the experimental data were extrapolated using a visually estimated shape of the DCS and the overall cross-section signal was numerically integrated. In order to estimate possible extrapolation errors on the ICSs estimated, the DCSs were also flat extrapolated to small and large θ using the extreme experimental DCSs and similarly integrated. The difference between the standard extrapolated ICSs and the flat-extrapolated ICSs did not exceed 6%. Uncertainties in the MSP values arise from several contributions, both statistical and systematic. When calculating the overall error from the measured data, we included errors from the experiment itself (DCS errors [1,2]) as well as in conversion of the spectra from TOF to E_L spectra. The combined error in the evaluation of MSP error contributions from H_2 elastic and inelastic DCSs averaged error over all angles ranges from 13% to 17%, and the angle-extrapolation procedure's error of the DCSs to small and large θ ranged from 1% to 6%. The determined error was 1% to 3%. These errors were added in quadrature to yield overall errors which range from 14% to 18%. Present values of $\langle E_L \rangle$ and MSP are presented in Table I.

TABLE I. Present values of MSP and $\langle E_L \rangle$ with one-standard-deviation errors as a function of E_0.

E_0 (eV)	$\langle E_L \rangle$ (eV)	Error	MSP (MeV cm^2/g)	Error
11.0	9.9	1.6	129.6	22.2
11.5	10	1.6	129.9	21.9
12.0	9.8	1.7	144.3	25.7
12.5	10.1	1.6	201.5	32.3
13.5	10.2	1.6	206.8	33.2
14.0	10.5	1.5	242.2	34.3
15.0	11.3	1.7	284.8	42.7
15.5	10.9	1.8	276.4	45.3
16.0	11	1.8	294.4	49.3
17.5	11.4	1.9	337.4	55.2
20.0	11.9	2.1	439.9	77.7
25.0	12.9	2.2	664.6	109.9

IV. RESULTS AND DISCUSSION

Theoretical evaluations of the electron MSP on H_2 have been conducted by many research groups. For the low-energy region, just above the threshold energy of the opening of the excitation channels, there are theoretical approaches predicting the MSP. However, there are still significant discrepancies between them. In Fig. 3, we compare the present values of the $\langle E_L \rangle$ for electron scattering from the ground state of H_2 with the available theoretical values [18] and the only available experimental values [25]. Figure 4 compares the present MSP results with the other available measurement and available calculations for H_2 found in the literature. A discussion of these now follows.

The theoretical CCC results of Fursa *et al.* [18] are expected to be the best low- to high-E_0 calculations, and the present experimental MSPs agree excellently with them, which indicates a positive result for our MSP values. Sugiyama [28] used the well-known high-energy Bethe-Bloch formula for electron straggling in foils and was implemented for the E_0 range from 20 eV to very high-E_0 values in the 10^4 eV region. Their work seems better suited to higher-E_0 values above those of the present work, as they fall well below the present results in the low-E_0 range. Similarly, the semiempirical formula of Peterson and Green [32] based on

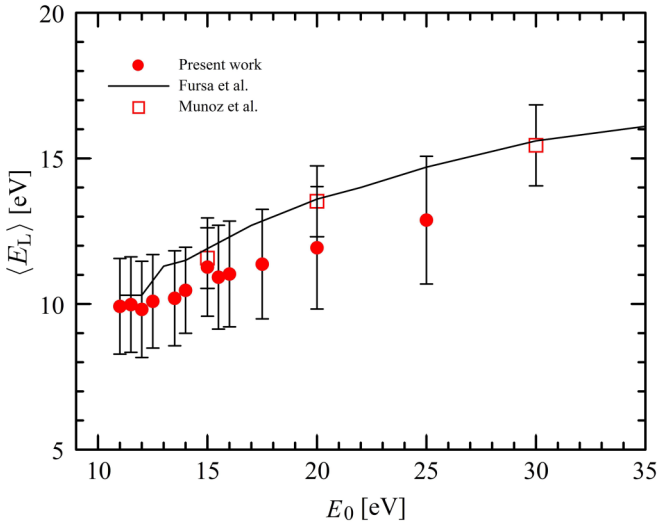

FIG. 3. $\langle E_L \rangle$ values as a function of E_0. Shown are the most recent theoretical values of Fursa *et al.* [18] and the only available experimental data of Munoz *et al.* [25]. See text for discussion.

aurora dynamics and using available cross sections for H_2, and along with the theoretical estimate of Spencer and Pol [31] from cross sections in the literature, gives a direct comparison with the present work only above 20 eV. Out of these three, the Spencer and Pol model more closely follows the present measurements. Peterson and Green's MSP values lie significantly higher than the present values. The work of Miles *et al.* [35] is similar to Sugiyama's [28] as it also uses the Bethe-Born approximation and generalized oscillator strengths derived from the excitation of H_2 and falls somewhat below the present MSPs. Interestingly, for $E_0 < 18$ eV, their MSPs rise well above the present experimental values after crossing the present results at $E_0 = 18$ eV. Another theoretical estimation was performed by Gumus [29], again using the Bethe-Born method, but with statistical charge distributions for the target electrons' structure, and offers an improved agreement for E_0 from 12.5–20 eV. As a note, the data of Gumus are incorrectly represented in the paper of Fursa *et al.* [18] because of Fursa *et al.* improperly calibrating Gumus' *y*-logarithmic scale in their digitizing software. Dalgarno and co-workers [34] used the well-known ionization formula of Opal *et al.* [40] and a good survey of excitation cross sections for H_2 to produce their MSP. Their results and those of Fursa *et al.* [18] give the best overall agreement with our MSPs. The estimates of the MSP obtained by Takayanagi and Nakata [33] were digitally retrieved from [18]. These greatly overestimate most of the MSPs in Fig. 4 and they are therefore significantly higher than other theoretical estimates. In the present energy range, there is disagreement with the low-E_0 points of the experimental MSPs of Munoz *et al.* [25]. However, as stated by Fursa *et al.* [18], these data require further normalization and, furthermore, they do not take into account the important inclusion of continuum electrons in their energy-loss spectra at higher-E_0 values, and thus result in raised MSP values. This fact can be seen in that their $\langle E_L \rangle$ are also higher than ours in Fig. 3 as a result of this or their transmission, or both. The procedure of deriving the mean excitation energy from the measured energy-loss spectra used by Munoz *et al.* was based on the estimation of the total and elastic cross sections. Both values come with their own uncertainties. Importantly, the significant discrepancy between our MSP values and the experimental values of Munoz *et al.* is clearly observed for $E_0 < 25$ eV when compared with the present experimental work. Thus, one must consider the present experimental values to be a useful improvement of the experimental MSP situation.

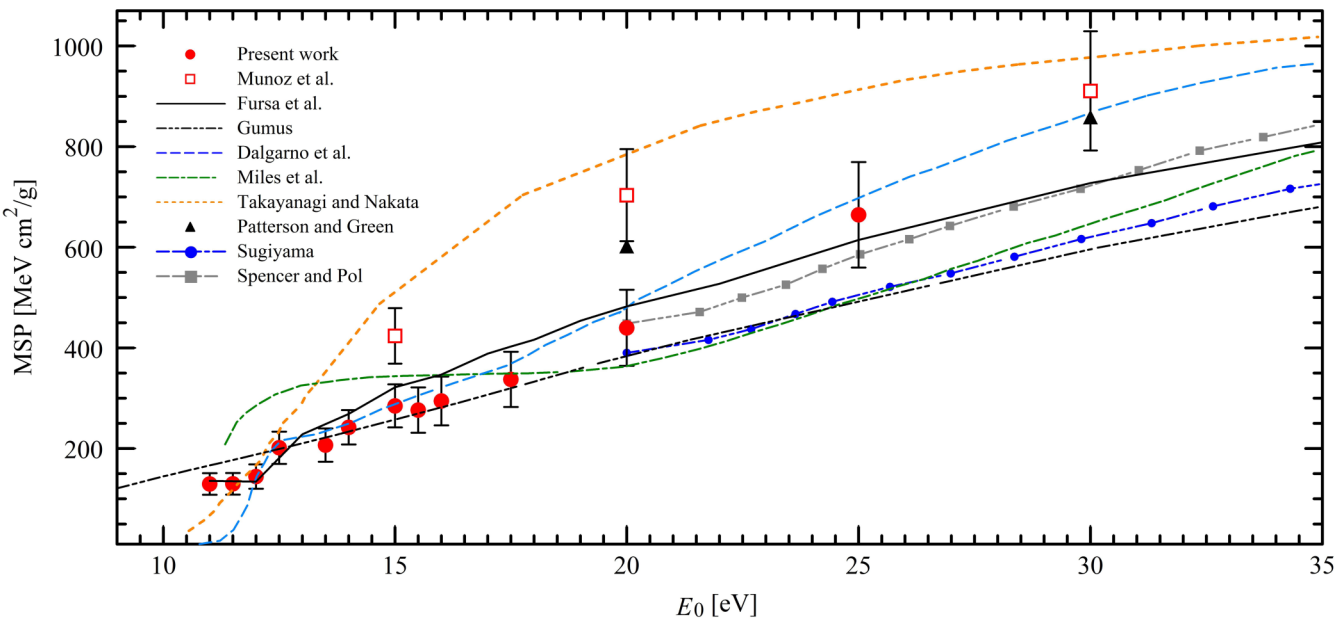

FIG. 4. MSP for electron scattering from the ground state of H_2. Experiment: Munoz *et al.* [25]; theory: Fursa *et al.* [18], Gumus [29], Dalgarno *et al.* [34], Miles *et al.* [35], Takayanagi and Nakata [33], Peterson and Green [32], Sugiyama [28], and Spencer and Pol [31]. See text for discussion.

V. CONCLUSIONS

Improved transmission-free energy-loss spectra of electrons were derived from TOF spectra measured with a TOF experimental setup [1,2]. From integral inelastic cross sections, determined from the spectra by normalizing the TOF elastic feature to our earlier accurate elastic cross sections of Muse *et al.* [39], the inelastic electron scattering DCSs for H_2 [2] were obtained. From this mean inelastic energy loss, $\langle E_L \rangle$ values were determined, resulting in the values of MSP for electron scattering from H_2. The present low-energy MSPs are found to be in best agreement with the CCC of Fursa *et al.* [18] and Dalgarno *et al.* [34], but in relative disagreement with the only other experimental MSP of Munoz *et al.* [25]. We note that this low-E_0 theoretical work of [18] is important as it extends the theoretical MSP values to energies below those of the Bethe-Born and Bethe-Bloch models undertaken at high-E_0 values. In terms of experiment, proper treatment of ionization has to be given in energy-loss spectra to prevent "double counting" of scattered and continuum electrons, which cannot be distinguished by either conventional electrostatic spectrometers (used in Ref. [25]) or TOF spectrometers such as ours [1,2]. However, a rough division of the ionization continuum by half in our TOF spectra is found to viably improve the situation as far as determining MSP is concerned when the ionization continuum is included, as is detailed in [2]. At higher-E_0 values, above the range of this work, we expect that the contribution to the energy-loss spectrum of the ionization continuum must increase and that this ionization contribution will be more severe, i.e., rising to $\gg$, than the 25% amount.

ACKNOWLEDGMENTS

M.A.K. and M.Z. acknowledge support from a National Science Foundation research Grant No. NSF-RUI-PHY 1606905. The authors thank M. C. Zammit (Los Alamos National Laboratory) and D. V. Fursa (Curtin University, Australia) for providing their tabulated data, valuable comments, and important discussions. M.Z. acknowledges financial support of the Fulbright Program to conduct this work at California State University Fullerton.

[1] M. Zawadzki, R. Wright, G. Dolmat, M. F. Martin, L. Hargreaves, D. V. Fursa, M. C. Zammit, L. H. Scarlett, J. K. Tapley, J. S. Savage, I. Bray, and M. A. Khakoo, Phys. Rev. A **97**, 050702(R) (2018).

[2] M. Zawadzki, R. Wright, G. Dolmat, M. F. Martin, B. Diaz, L. Hargreaves, D. Coleman, D. V. Fursa, M. C. Zammit, L. H. Scarlett, J. K. Tapley, J. S. Savage, I. Bray, and M. A. Khakoo, Phys. Rev. A **98**, 062704 (2018).

[3] L. R. LeClair and S. Trajmar, J. Phys. B **25**, 5543 (1996).

[4] A. L. Hughes and J. H. McMillen, Phys. Rev. **41**, 39 (1932).

[5] L. H. Scarlett, J. K. Tapley, D. V. Fursa, M. C. Zammit, J. S. Savage, and I. Bray, Eur. Phys. J. D **72**, 34 (2018).

[6] J. K. Tapley, L. H. Scarlett, J. S. Savage, D. V. Fursa, M. C. Zammit, and I. Bray, Phys. Rev. A **98**, 032701 (2018).

[7] M. C. Zammit, J. S. Savage, D. V. Fursa, and I. Bray, Phys. Rev. A **95**, 022708 (2017).

[8] J. K. Tapley, L. H. Scarlett, J. S. Savage, M. C. Zammit, D. V. Fursa, and I. Bray, J. Phys. B **51**, 144007 (2018).

[9] J. P. Boeuf, G. J. M. Hagelaar, P. Sarrailh, G. Fubiani, and N. Kohen, Plasma Sources Sci. Technol. **20**, 015002 (2016).

[10] B. Boudaïffa, P. Cloutier, D. Hunting, M. A. Huels, and L. Sanche, Science **287**, 1658 (2000).

[11] X. Pan, P. Cloutier, D. Hunting, and L. Sanche, Phys. Rev. Lett. **90**, 208102 (2003).

[12] O. Zatsarinny and K. Bartschat, J. Phys.: Conf. Ser. **488**, 012044 (2014).

[13] I. Bray, D. V. Fursa, A. S. Kheifets, and A. T. Stelbovics, J. Phys. B **35**, R117 (2002).

[14] D. A. Horner, C. William McCurdy, and T. N. Rescigno, Phys. Rev. A **71**, 012701 (2005).

[15] M. C. Zammit, J. S. Savage, D. V. Fursa, and I. Bray, Phys. Rev. Lett. **116**, 233201 (2016).

[16] J. Carr, P. Galiatsatos, J. Gorfinkiel, A. Harvey, M. Lysaght, D. Madden, Z. Masin, M. Plummer, J. Tennyson, and H. Varambhia, Eur. Phys. J. D **66**, 1 (2012).

[17] R. F. da Costa, M. T. do N. Varella, M. H. F. Bettega, and M. A. P. Lima, Eur. Phys. J. D **69**, 159 (2015).

[18] D. V. Fursa, M. C. Zammit, R. L. Threlfall, J. S. Savage, and I. Bray, Phys. Rev. A **96**, 022709 (2017).

[19] I. I. Fabrikant, S. Eden, N. J. Mason, and J. Fedor, Adv. At. Mol. Opt. Phys. **66**, 545 (2017).

[20] M. Zawadzki, M. Ranković, J. Kočišek, and J. Fedor, Phys. Chem. Chem. Phys. **20**, 6838 (2018).

[21] M. Zawadzki, M. Čížek, K. Houfek, R. Čurík, M. Ferus, S. Civiš, J. Kočišek, and J. Fedor, Phys. Rev. Lett. **121**, 143402 (2018).

[22] P. Mayles, A. Nahum, and J. C. Rosenwald, *Handbook of Radiotherapy Physics: Theory and Practice* (CRC, Boca Raton, FL, 2007).

[23] B. J. McFarland, *Nuclear Medicine Radiation Dosimetry: Advanced Theoretical Principles* (Springer, Berlin, 2010).

[24] J. L. Fox, M. I. Galand, and R. E. Johnson, Space Sci. Rev. **139**, 3 (2008).

[25] A. Munoz, J. C. Oller, F. Blanco, J. D. Gorfinkiel, and G. García, Chem. Phys. Lett. **433**, 253 (2007).

[26] H. Bethe and W. Heitler, Proc. R. Soc. Series A. **146**, 83 (1934).

[27] M. Born, Z. Phys. **38**, 803 (1926).

[28] H. Sugiyama, Phys. Med. Biol. **30**, 331 (1985).

[29] H. Gumus, Radiat. Phys. Chem. **72**, 7 (2005).

[30] F. Rohrlich and B. C. Carlson, Phys. Rev. **93**, 38 (1954).

[31] L. V. Spencer and R. Pol, National Bureau of Standards, Report No. NBSIR 78-1523, 1978.

[32] L. R. Peterson and A. E. S. Green, J. Phys. B: At. Mol. Phys. **1**, 1131 (1968).

[33] K. Takayanagi and K. Nakata, Bull. Inst. Space Aeronaut. Sci. **6**, 849 (1970).

[34] A. Dalgarno, M. Yan, and W. Liu, Astrophys. J. Suppl. **125**, 237 (1999).

[35] W. T. Miles, R. Thompson, and A. E. S. Green, J. Appl. Phys. **43**, 678 (1972).

[36] J. Liu, E. J. Salumbides, U. Hollenstein, J. C. J. Koelemeij, K. S. E. Eikema, W. Ubachs, and F. Merkt, J. Chem. Phys. **130**, 174306 (2009).

[37] M. Hughes, K. E. James, Jr., J. G. Childers, and M. A. Khakoo, Meas. Sci. Technol. **14**, 841 (1994).

[38] Avtech Electrosystems Ltd., Model No. AVR-E5-B-05, Ogdensburg, New York 13669, USA.

[39] J. Muse, H. Silva, M. C. A. Lopes, and M. A. Khakoo. J. Phys. B: At. Mol. Opt. Phys. **41**, 095203 (2008).

[40] C. B. Opal, W. K. Peterson, and E. C. Beaty, J. Chem. Phys. **55**, 4100 (1971).